

Multi-UAV trajectory planning problem using the difference of convex function programming

Anh Phuong Ngo¹, Christan Thomas², Ali Karimodini¹ and Hieu T. Nguyen¹

¹Dept. of Electrical & Computer Eng., North Carolina A&T State University, Greensboro, NC 27411, USA

²Dept. of Flight Test, Lockheed Martin Corporation, Fort Worth, TX 76108, USA

angol@aggies.ncat.edu, christan.thomas@lhco.com, {akarimod, htnguyen1}@ncat.edu

Abstract—This paper presents two different optimization-based trajectory generation methods for multiple aircrafts, i.e., mixed-integer convex programming (MICP) and difference of convex functions (DC) programming. Two methods deal with the aircraft separation constraint in different manners, which also leads to two different objective functions. The first involves a convex objective function while the second derives a non-convex objective function from the aircraft separation constraint, which has a non-convex nature. The numerical performance of two objective functions is explored and compared. For the same given aircraft starting points and destinations, the solution of the DCA facilitates to the aircrafts to consume as less fuel as the solution of MICP does. In addition, the advantage analysis of MICP and DCA compared to the standard method as well as the convergence analysis of DCA are also addressed.

Keywords—Trajectory planning, mixed-integer convex programming, non-convex programming, collision avoidance

NOMENCLATURE

A. Set and Indices

\mathcal{N}, i	Set and index of vehicles, $i \in \mathcal{N}$
\mathcal{T}, t	Set and index of time steps, $t = 1, 2, \dots, K \in \mathcal{T}$
S	Set of initial states, including starting position $\mathcal{S}(x_i^s, y_i^s, z_i^s)$, starting velocity $\mathcal{S}(v_i^x, v_i^y, v_i^z)$, and starting force $\mathcal{S}(f_i^x, f_i^y, f_i^z)$ of vehicle i
\mathcal{G}	Set of goal states, including goal position $\mathcal{G}(x_i^g, y_i^g, z_i^g)$, goal velocity $\mathcal{G}(v_i^x, v_i^y, v_i^z)$, and goal force $\mathcal{G}(f_i^x, f_i^y, f_i^z)$ of vehicle i

B. Parameters

\bar{x}, \underline{x}	Upper/lower limits of x -coordinate that vehicles can reach
\bar{y}, \underline{y}	Upper/lower limits of y -coordinate that vehicles can reach
\bar{z}, \underline{z}	Upper/lower limits of z -coordinate that vehicles can reach
$\bar{V}_i, \underline{V}_i$	Upper/lower limits of velocity of vehicle i
$\bar{F}_i, \underline{F}_i$	Upper/lower limits of force of vehicle i
d	Minimum distance among two vehicles to avoid a collision
\mathbf{A}_i	State-space matrix of vehicle i
\mathbf{B}_i	Input matrix of vehicle i
ρ^f	Penalty for O_f of objective function
ρ^k	Penalty for O_g of objective function

C. Variables

$x_{i,k}$	x -coordinate of position of vehicle i at time step k
$y_{i,k}$	y -coordinate of position of vehicle i at time step k
$z_{i,k}$	z -coordinate of position of vehicle i at time step k
$\mathcal{P}_{i,k}$	position of vehicle i at time step k in xyz coordinate
$v_{i,k}^x$	x -component of velocity vector of vehicle i at time step k
$v_{i,k}^y$	y -component of velocity vector of vehicle i at time step k
$v_{i,k}^z$	z -component of velocity vector of vehicle i at time step k
$\vec{V}_{i,k}$	velocity vector of vehicle i at time step k
$f_{i,k}^x$	x -component of force vector of vehicle i at time step k
$f_{i,k}^y$	y -component of force vector of vehicle i at time step k
$f_{i,k}^z$	z -component of force vector of vehicle i at time step k

$\vec{F}_{i,k}$
 $u_{i,j,k}^v$

force vector of vehicle i at time step k
Binary variable used to linearize the non-convex collision avoidance constraint

I. INTRODUCTION

Trajectory planning problem is aimed to find an optimal solution of trajectory for a single aircraft or a group of aircrafts to travel from a given starting state over a map of the environment to a goal state. Mixed-integer linear programming (MILP) is the standard method used to solve the trajectory generation problem for many decades [1]. MILP is a powerful optimization method that allows inclusion of integer variables and discrete logic of linearization for non-convex constraints in a continuous linear trajectory optimization [2], [3]. These mixed integer and continuous variables can be used to model logical constraints such as obstacle avoidance and vehicle separation, while the dynamic and kinematic settings of the aircrafts are casted in continuous constraints. Concurrently, the magnitude of velocity and force vectors are modelled by the spherical geometry-based sampling approximation technique for 3-D environment, or the edges of an N-sided polygon approximation technique for 2-D environment [4]. To this extent, MILP method uses many auxiliary variables and constraints to formulate the trajectory optimization problem.

The recent improvements in aircraft's capabilities, especially for unnamed aerial vehicles (UAVs), facilitate them to carry out longer and more complex missions in dynamic environments. Moreover, as more vehicles and more targets are involved in a mission, the size of the trajectory optimization problem based on MILP increases exponentially. Consequently, the computation time of the problem to obtain the optimal solution becomes much more expensive. Convex optimization methods can handle well the conic constraints such as bounds on the magnitude of velocity and force vectors without incorporating the approximation techniques [5]. This paper presents two effective convex programming (CP) methods, i.e., mixed-integer convex programming (MICP) and difference of convex algorithm (DCA). These methods formulate the convex constraints in the same manner, but there is a difference on how the former and latter approximate non-convex constraints of collision avoidance.

This paper is organized as follows: Section II and III present the mathematical formulations and algorithms of MICP and DCA, respectively. The mathematical advantage of MICP

and DCA over MILP is demonstrated in section IV, while the numerical results of our formulations and algorithms are shown in section V. Finally, section VI will conclude the paper and discuss possible future research.

II. STATE-SPACE SYSTEM MODELING OF AN UAV

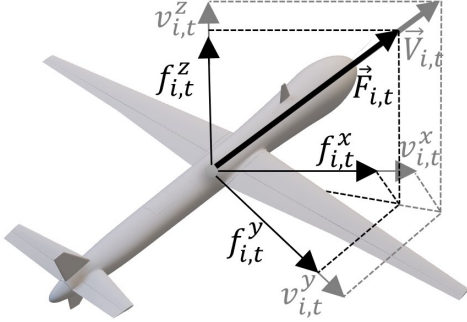


Fig. 1. Velocity and Force vectors in body and fixed axes coordinate system

We consider a fixed-wing UAV modelled as a point mass flying in a predetermined 3-dimensional space with the (x, y, z) coordinates (i.e., forward, side, and vertical directions respectively) as shown in Figure 1 where i denotes the index of UAV in the swarm at the location $(x_{i,t}, y_{i,t}, z_{i,t})$ and m_i is its constant mass. The UAV's velocity $\vec{V}_{i,t}$, by definition, represents the change of UAV's location as:

$$\vec{V}_{i,t} = \vec{v}_{i,t}^x + \vec{v}_{i,t}^y + \vec{v}_{i,t}^z = \frac{dx_i}{dt} + \frac{dy_i}{dt} + \frac{dz_i}{dt} \quad (1)$$

and can be decomposed into $\vec{v}_{i,t}^x = \frac{dx_i}{dt}$ (the forward velocity), $v_{i,t}^y = \frac{dy_i}{dt}$ (the side velocity), and $v_{i,t}^z = \frac{dz_i}{dt}$ (the vertical velocity). The force $\vec{F}_{i,t}$ as the control input alternates the UAV acceleration following Newton's second law:

$$\vec{F}_{i,t} = m_i \frac{d(\vec{V}_{i,t})}{dt} = m_i \left(\frac{d\vec{v}_{i,t}^x}{dt} + \frac{d\vec{v}_{i,t}^y}{dt} + \frac{d\vec{v}_{i,t}^z}{dt} \right), \quad (2)$$

which is also decomposed into $\vec{f}_{i,t}^x = \frac{d\vec{v}_{i,t}^x}{dt}$, $\vec{f}_{i,t}^y = m_i \frac{dv_{i,t}^y}{dt}$, and $\vec{f}_{i,t}^z = m_i \frac{dv_{i,t}^z}{dt}$ (i.e., forward, side, vertical forces).

Equations (1)-(2) together form the following UAV's kyno-dynamic state-space model:

$$\frac{d\mathbf{X}_{i,t}}{dt} = \mathbf{A}\mathbf{X}_{i,t} + \mathbf{B}\mathbf{U}_{i,t} \quad (3)$$

where $\mathbf{X}_{i,t} = [x_{i,t}, y_{i,t}, z_{i,t}, v_{i,t}^x, v_{i,t}^y, v_{i,t}^z]^\top$,

$$\mathbf{U}_{i,t} = [f_{i,t}^x, f_{i,t}^y, f_{i,t}^z]^\top,$$

$$\mathbf{A}_i = \begin{pmatrix} 0 & 0 & 0 & 1 & 0 & 0 \\ 0 & 0 & 0 & 0 & 1 & 0 \\ 0 & 0 & 0 & 0 & 0 & 1 \\ 0 & 0 & 0 & 0 & 0 & 0 \\ 0 & 0 & 0 & 0 & 0 & 0 \\ 0 & 0 & 0 & 0 & 0 & 0 \end{pmatrix}, \mathbf{B}_i = \frac{1}{m_i} \begin{pmatrix} 0 & 0 & 0 \\ 0 & 0 & 0 \\ 0 & 0 & 0 \\ 1 & 0 & 0 \\ 0 & 1 & 0 \\ 0 & 0 & 1 \end{pmatrix}$$

Here $\mathbf{X}_{i,t}$ denotes the state variable vector, $\mathbf{U}_{i,t}$ denotes the control input, \mathbf{A}_i denotes the state matrix, and \mathbf{B}_i denotes the input matrix of UAV i . The kyno-dynamic model (3) can be converted into the discrete time-variant form as follows:

$$\mathbf{X}_{i,k+1} = \hat{\mathbf{A}}_i \mathbf{X}_{i,k} + \hat{\mathbf{B}}_i \mathbf{U}_{i,k}, \quad \forall i \in \mathcal{N}, \forall k \in \mathcal{T}, \quad (4)$$

where $\hat{\mathbf{A}}_i = \mathbf{I} + \Delta T \mathbf{A}_i$, $\hat{\mathbf{B}}_i = \Delta T \mathbf{B}_i$, particularly:

$$\hat{\mathbf{A}}_i = \begin{pmatrix} 1 & 0 & 0 & \Delta T & 0 & 0 \\ 0 & 1 & 0 & 0 & \Delta T & 0 \\ 0 & 0 & 1 & 0 & 0 & \Delta T \\ 0 & 0 & 0 & 1 & 0 & 0 \\ 0 & 0 & 0 & 0 & 1 & 0 \\ 0 & 0 & 0 & 0 & 0 & 1 \end{pmatrix}, \hat{\mathbf{B}}_i = \frac{\Delta T}{m_i} \begin{pmatrix} 0 & 0 & 0 \\ 0 & 0 & 0 \\ 0 & 0 & 0 \\ 1 & 0 & 0 \\ 0 & 1 & 0 \\ 0 & 0 & 1 \end{pmatrix},$$

and $\mathbf{X}_{i,k} = [x_{i,k}, y_{i,k}, z_{i,k}, v_{i,k}^x, v_{i,k}^y, v_{i,k}^z]^\top$ and $\mathbf{U}_{i,k} = [f_{i,k}^x, f_{i,k}^y, f_{i,k}^z]^\top$ respectively represent vectors of state variables and control inputs of UAV i at time step k , and ΔT is the length of the time step.

III. MULTI-UAV TRAJECTORY PLANNING PROBLEM

We consider the trajectory planning problem for a swarm of N UAVs in which each UAV needs to travel from its initial position to the final destination without colliding with other UAVs. In other words, for each UAV $i \in \mathcal{I}$ in the swarm, we need to determine a sequence of positions $(x_{i,k}, y_{i,k}, z_{i,k})$ forming the UAV's trajectory and the sequence of control action $\mathbf{U}_{i,k}$ at each time step $k \in \mathcal{T}$ such that the UAV reaches its final destination without collision with others. This can mathematically formulated as a large scale non-convex optimization problem as follows:

$$\min_{\mathbf{X}, \mathbf{U}} \sum_{i=1}^N \sum_{k=1}^K \left(\rho^f \times \underbrace{\sqrt{(f_{i,t}^x)^2 + (f_{i,t}^y)^2 + (f_{i,t}^z)^2}}_{O_f} + \rho^k \times \underbrace{\sqrt{(x_{i,t} - x_i^g)^2 + (y_{i,t} - y_i^g)^2 + (z_{i,t} - z_i^g)^2}}_{O_g} \right), \quad (5)$$

subject to:

$$(\mathbf{X}_i, \mathbf{U}_i) \in \Omega_i = \left\{ \mathbf{X}_{i,k+1} = \hat{\mathbf{A}}_i \mathbf{X}_{i,k} + \hat{\mathbf{B}}_i \mathbf{U}_{i,k}, \quad \forall k, \right. \quad (6a)$$

$$(x_{i,1}, y_{i,1}, z_{i,1})^\top = (x_i^S, y_i^S, z_i^S)^\top, \quad (6b)$$

$$(v_{i,1}^x, v_{i,1}^y, v_{i,1}^z)^\top = (v_{i,1}^{x,S}, v_{i,1}^{y,S}, v_{i,1}^{z,S})^\top, \quad (6c)$$

$$(x_{i,K}, y_{i,K}, z_{i,K})^\top = (x_i^G, y_i^G, z_i^G)^\top, \quad (6d)$$

$$(v_{i,K}^x, v_{i,K}^y, v_{i,K}^z)^\top = (v_{i,K}^{x,G}, v_{i,K}^{y,G}, v_{i,K}^{z,G})^\top, \quad (6e)$$

$$(f_{i,K}^x, f_{i,K}^y, f_{i,K}^z)^\top = (f_{i,K}^{x,G}, f_{i,K}^{y,G}, f_{i,K}^{z,G})^\top, \quad (6f)$$

$$\sqrt{(v_{i,k}^x)^2 + (v_{i,k}^y)^2 + (v_{i,k}^z)^2} \leq \bar{V}_i, \quad \forall k \quad (6g)$$

$$\sqrt{(f_{i,k}^x)^2 + (f_{i,k}^y)^2 + (f_{i,k}^z)^2} \leq \bar{F}_i, \quad \forall i. \quad (6h)$$

$$\sqrt{(x_{i,k} - x_{j,k})^2 + (y_{i,k} - y_{j,k})^2 + (z_{i,k} - z_{j,k})^2} \geq d, \quad \forall i \neq j, \forall t. \quad (7)$$

In the objective function (11), we want to minimize the control effort and the traveling time of UAVs of reaching their final destination. The objective consists of two terms, O_f penalizes the force supplying to vehicle i at time t with a unit fuel cost ρ_1 whereas O_g penalizes the remaining distance of each vehicle i to its goal position multiplying with the value ρ^k . Typically, ρ^k is set as the increasing function of the time indexes, e.g., $\rho^k := a \times k$, $a > 0$, so O_g urges UAVs to reach their goal points as soon as possible. The objective function is subject to two sets of constraints as follows.

Constraint (6) encapsulates all local constraints state variables and control inputs of individual UAVs $i = 1, \dots, N$ in their corresponding feasible set Ω_i . In particular, the dynamics of each vehicle following discrete-time and linear state-space equation (4) is now acts as linear constraint (6a). The starting position is expressed in (6b)-(6c) whereas the set of final conditions including the goal position, velocity, and force of vehicle are introduced in (6d)-(6f). The physical limits of UAV's velocity and driving force are captured in (6g) and (6h). The feasible set Ω_i is convex and (6) is a convex constraint.

Constraint (7) represents the collision avoidance among UAVs in the pair. In particular, the Euclidean separation distance between all pairs of vehicles $i \neq j$ must be equal or greater than the safety margin d at all time step $k = 1, \dots, K$. The number of collision avoidance conditions is $\frac{N \times (N-1)}{2} \times K$. Since the Euclidean distance norm is a convex function, (7) is a non-convex constraint.

Overall, the multi UAVs' trajectory planning problem can be summarized in the following form:

$$\begin{aligned} \text{[P]} \quad \min \quad & O_f + O_g \\ \text{s.t.} \quad & (\mathbf{X}_i, \mathbf{U}_i) \in \Omega_i, \forall i, \\ & \text{non-convex collision avoidance (7).} \end{aligned}$$

It is worth mentioning that Problem P is generic as we can tailor Ω_i or the objective function for different application requirements, e.g., the UAV's trajectory must visit certain locations or stay close as much as possible for certain pre-determined paths. Such modifications generally do not affect the convexity of Ω_i , thus not affecting computational performance. The complexity of P stems from a large number of nonconvex collision avoidance conditions (7). Such constraint, however, is critical for safety requirements and cannot be ignored. The aim of this paper is to tackle this convex constraint set, thus facilitating the computation of UAV swarm coordination in the form of P.

IV. MIXED-INTEGER CONVEX PROGRAMMING MODEL

We can use mixed integer linear programming to capture the nonconvexity constraint. Without loss of generality, a generic nonconvex constraint can be written in the form $x \notin \mathcal{C}$ where

\mathcal{C} is a convex set of variable x . If we can polyhedrally outer approximate \mathcal{C} by a set of L linear constraints

$$\mathbf{Poly}(\mathcal{C}) = \left\{ x \mid a_\nu^\top x \leq b_\nu, \nu = 1, 2, \dots, L \right\}, \quad (8)$$

then the condition $x \notin \mathcal{C}$ will be attained by letting at least one constraint in (8) be violated by introducing binary variable u_m as follows:

$$a_\nu^\top x \geq b_\nu + \epsilon - \bar{U}u_\nu, \quad u_\nu \in \{0, 1\}, \quad \forall m = 1, 2, \dots, M, \\ \sum_{\nu=1}^M (1 - u_\nu) \geq 1 \quad (9)$$

where \bar{U} is a sufficient large number and ϵ is a small number. Constraint (9) means that at least one value of $u_\nu = 0$, consequently, one inequality $a_\nu^\top x \geq b_\nu + \epsilon$ activates, forcing $x \notin \mathcal{C}$ (the term ϵ is used to prevent the equality $a_\nu^\top x = b_\nu$).

Note that we can approximate the 2-D Lorentz cone:

$$\mathbb{L}^2 = \left\{ (\hat{x}, \hat{y}, d) \in \mathbb{R}^2 \times \mathbb{R}_+ \mid \sqrt{\hat{x}^2 + \hat{y}^2} \leq d \right\}$$

by the following linear inequalities of variables α, β :

$$\alpha_0 \geq \hat{x}, \quad \alpha_0 \geq -\hat{x}, \quad \beta_0 \geq \hat{y}, \quad \beta_0 \geq -\hat{y}, \quad (10a)$$

$$\left\{ \beta_{\nu+1} \geq -\sin\left(\frac{\pi}{2^\nu}\right) \alpha_\nu + \cos\left(\frac{\pi}{2^\nu}\right) \beta_\nu, \quad (10b) \right.$$

$$\left. \beta_{\nu+1} \geq \sin\left(\frac{\pi}{2^\nu}\right) \alpha_\nu - \cos\left(\frac{\pi}{2^\nu}\right) \beta_\nu, \quad (10c) \right.$$

$$\left. \alpha_{\nu+1} = \cos\left(\frac{\pi}{2^\nu}\right) \alpha_\nu + \sin\left(\frac{\pi}{2^\nu}\right) \beta_\nu, \right\} \quad (10d)$$

$$\nu = 0, \dots, L-1,$$

$$\alpha_L \leq d, \quad \beta_L \leq \tan\left(\frac{\pi}{2^L}\right) \alpha_L, \quad (10e)$$

The approximation (10) basically forms a regular 2^L -sided polygon with $2(L+1)$ additional variables $\alpha_\nu, \beta_\nu, \nu = 1, \dots, L$ as follows:

$$\mathbf{Poly}(\mathbb{L}^2) = \left\{ (\hat{x}, \hat{y}, \alpha, \beta) \in \mathbb{R}^2 \times \mathbb{R}^{2(L+1)} \mid (10a) - (10e) \right\},$$

Note also that the collision condition, i.e., the distance between two UAV is less than d , is in the form of 3-dimension Lorentz cone \mathbb{L}^3

$$\mathbb{L}^3 = \left\{ (\hat{x}, \hat{y}, \hat{z}, d) \in \mathbb{R}^2 \times \mathbb{R}_+ \mid \sqrt{\hat{x}^2 + \hat{y}^2 + \hat{z}^2} \leq d \right\},$$

that can be captured by two second-order cone constraints:

$$\hat{x}^2 + \hat{y}^2 \leq \hat{w}^2, \quad \hat{w}^2 + \hat{z}^2 \leq d^2, \quad \hat{w} \geq 0,$$

each is indeed \mathbb{L}^2 and can be polyhedrally approximated using (10). Consequently, we can combine (9) and (10) to construct a set of MILP constraints enforcing the distance between two UAVs outside the collision range. In particular, we need to write two sets of linear constraints (10) associated with the polyhedral approximation $\mathbf{Poly}(\mathbb{L}^2)$ of two 2-D Lorentz cones in the standard form (8) and then apply the MILP reformulation trick (9). Due to page limitation, we omit the presentation of the general case with arbitrary L . In the special

case $L = 2$, we can compact the set of constraints as follows:

$$x_{i,k} - x_{j,k} \geq d - \bar{U}u_{i,j,k}^1, x_{j,t} - x_{i,k} \geq d - \bar{U}u_{i,j,k}^2 \quad (11a)$$

$$y_{i,k} - y_{j,k} \geq d - \bar{U}u_{i,j,k}^3, y_{j,k} - y_{i,k} \geq d - \bar{U}u_{i,j,k}^4 \quad (11b)$$

$$z_{i,k} - z_{j,k} \geq d - \bar{U}u_{i,j,t}^5, z_{j,k} - z_{i,k} \geq d - \bar{U}u_{i,j,k}^6 \quad (11c)$$

$$\sum_{\nu=1}^6 u_{i,j,k}^{\nu} \leq 5, \forall k, \forall i \neq j. \quad (11d)$$

which enforces the distance of two UAVs i and j outside the cubic outerly approximating the collision sphere of radius d , i.e., $|x_{i,k} - x_{j,k}| \geq d$ OR $|y_{i,k} - y_{j,k}| \geq d$ OR $|z_{i,k} - z_{j,k}| \geq d$, $\forall k, \forall i \neq j$. (ϵ in (9) is chosen as zero since the distance d satisfies the minimum requirement of safety).

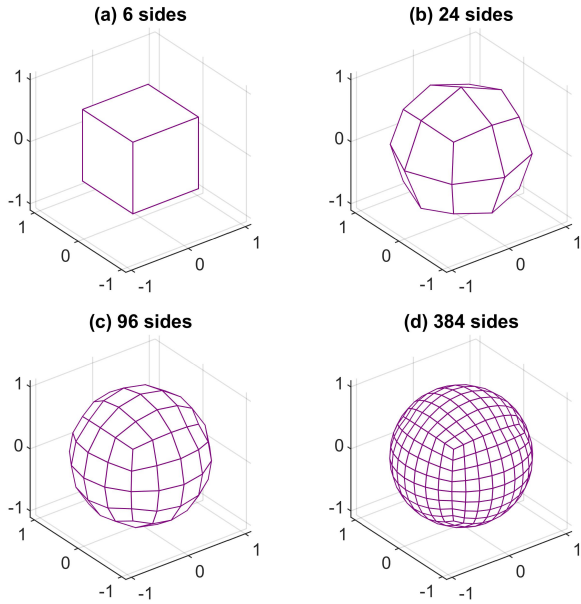


Fig. 2. A polyhedral approximation of the 3-D ball

Remark: Figure 2 represents a polyhedral approximation of the 3-D ball with radius d . While the approximation error reduces as L increases, the computational demand significantly increases as the number of constraints and binary variables employed increases. Indeed, our examination shows that only $L = 2$ is computationally feasible given the number of collision avoidance conditions that we need to approximate is $\frac{N \times (N-1)}{2} \times K$. However, MILP reformulation with $L = 2$ is very conservative, which might result in infeasibility if we coordinate a large swarm of UAVs in a small space.

V. DIFFERENCE OF CONVEX ALGORITHM

A. Difference of Convex Programming

The difference of convex (DC) programming plays an important role in solving a class of non-convex problems. The

problem candidates must strictly comply the following form:

$$\begin{aligned} & \min f_0(x) - g_0(x) \\ & \text{subject to } f_i(x) - g_i(x) \leq 0, \quad i = 1, 2, \dots, m, \\ & \quad \quad \quad h_j(x) \leq 0, \quad j = 1, 2, \dots, c, \end{aligned} \quad (12)$$

where $x \in \mathbb{R}^n$ is the decision variable; $h_j : \mathbb{R}^n \rightarrow \mathbb{R}$, $f_i : \mathbb{R}^n \rightarrow \mathbb{R}$ and $g_i : \mathbb{R}^n \rightarrow \mathbb{R}$ are convex; and f_0 and g_0 are affine [6]. One of the most widely-used techniques for DC programming is the DC algorithm (DCA) [7], which is a scalable approach and applicable to many large-scale (smooth or nonsmooth) non-convex programs. Although DCA has a local character of heuristic methods, it has been observed to often converge to the global optimum. Furthermore, DCA has been proved to be more robust and efficient than conventional methods [8], [9]. DCA also has a different name known as the convex-concave procedure (CCP). Its general idea is to first rewrite the non-convex objective function and/or non-convex constraints into the form of (12). Afterwards, the CCP convexify the concave expressions “ $-g_0(x)$ ” and “ $-g_i(x)$ ” into convex expressions “ $g_0(x)$ ” and “ $g_i(x)$ ”, and then call the available solvers to work out on the reformulated convexified sub-problems. To this extent, CCP can utilize the capability of available convex optimization solvers [10] to find optimal solution for the non-convex problem.

Penalty CCP is an extension of CCP, which accommodates infeasible initial points. Penalty CCP relaxes the constraint violations by adding slack variable s_i as well as imposing an increasing penalty τ_k for summation of the violations to the objective function [10]. The algorithmic detail of penalty CCP is given as below:

Algorithm 1 Penalty CCP [6]

given an initial point $x_0, 0 > 0, \tau_{max} > 0$, and $\mu > 1$.
 $k := 0$

repeat

1. *Convexify.* Form $\hat{g}_i(x, x_k) = g_i(x_k) + \nabla g_i(x_k)^\top (x - x_k)$ for $i = 0, \dots, m$.

2. *Solve.* Set the value of x_{k+1} to a solution of

$$\min f_0 - \hat{g}_0(x, x_k) + \tau_k \sum_{i=1}^m s_i$$

Subject to:

$$f_i(x) - \hat{g}_i(x, x_k) \leq s_i, \quad i = 1, 2, \dots, m,$$

$$s_i \geq 0, \quad i = 1, 2, \dots, m,$$

$$h_j(x) \leq 0, \quad j = 1, 2, \dots, c.$$

3. *Update* τ . $\tau_{k+1} := \min(\mu\tau_k, \tau_{max})$

4. *Update iteration.* $k := k + 1$

until stopping criterion is satisfied.

Stopping criterion is one of two below conditions satisfied:

- 1) τ_k (the trade-off penalty between satisfying the constraints and minimizing the objective) equals to τ_{max} (the upper bound of τ_k value) expressed as follows:

$$\tau_k = \tau_{max}$$

At each iteration k , τ_k can increase a rate of geometric progression μ . It is also worth noting that selecting larger τ_k value is on the side of satisfying the constraints.

- 2) The solving reformulated convexified sub-problem is very small demonstrated as follows:

$$\delta_k = \left(f_0(x_k) - g_0(x_k) + \tau_k \sum_{i=1}^m s_i^k \right) - \left(f_0(x_{k+1}) - g_0(x_{k+1}) + \tau_k \sum_{i=1}^m s_i^{k+1} \right) \leq \epsilon,$$

where s_i^k is a slack variable associated with constraint i found at iteration k and either x_k is feasible specified as

$$\sum_{i=1}^k s_i^{k+1} \leq \epsilon_{\text{violation}} \approx 0.$$

B. Disciplined Convex Programming

Most of common convex solvers (e.g. MOSEK, GUROBI, CPLEX, etc.) are developed to handle certain structures of convex programming defined as *standard forms*. A mathematical model has to go through the checking process of whether or not the model is convex and comply the standard forms. However, this task is proved to be theoretically intractable. In addition, the solvers could falsely reject a possible convex programming model. Disciplined convex programming (DCP) is a methodology of constructing convex optimization models in form of mathematical expressions with known curvature from well-investigated base functions [11]. Using conventions from the collection of DCP to build mathematical program is guaranteed to be convex and fall in standard forms of the solvers. Therefore, DCP can simplify the verification step by solvers for a mathematical model.

C. Disciplined Convex-concave Programming

Disciplined convex-concave programming (DCA) is a combination version of CCP and DCP. Before DCA decomposes the non-convex objective function and/or non-convex constraints as same as CPP, DCA enforces all expressions in the non-convex functions to comply with the standard forms of DCP. On this wise, the reformulated convexified sub-problems after the decomposition process can be guaranteed to be convex and then solved by solvers.

D. Problem Reformulation

$$\min \sum_{t \in \mathcal{T}} \left(\sum_{i \in \mathcal{N}} \left(\rho_1 \times \underbrace{\sqrt{(f_{i,t}^x)^2 + (f_{i,t}^y)^2 + (f_{i,t}^z)^2}}_{O_1} + t \times \underbrace{\sqrt{(x_{i,t} - x_i^g)^2 + (y_{i,t} - y_i^g)^2 + (z_{i,t} - z_i^g)^2}}_{O_2} \right) - \rho_2 \sum_{i,j \in \mathcal{N}} \underbrace{\sqrt{(x_{i,t} - x_{j,t})^2 + (y_{i,t} - y_{j,t})^2 + (z_{i,t} - z_{j,t})^2}}_{O_3} \right) \quad (13a)$$

TABLE I
GRAND TOTAL FUEL COST OF VEHICLES IN MICP AND DCA

	MICP	DCP	$\Delta(\text{MICP} - \text{DCP})$
5 vehicles	326.18	323.17	3.01
10 vehicles	1594.11	1592.32	1.79
15 vehicles	2855.25	2839.97	15.28

As can be seen, the objective function (13a) is non-convex as it contains a concave expression. The penalty CCP algorithm is utilized in our trajectory planning problem by defining:

$$\begin{cases} f_0 = O_1 + O_2, & \text{convex expressions} \\ -g_0 = -O_3, & \text{concave expression} \end{cases}$$

for the objective function (13a). It is noted that ρ_2 should be adjusted along with the number of vehicles. As the value of O_3 would increase exponentially as long as the number of pairs of vehicles $\binom{N}{2}$ increases. The safety distance satisfaction between positions $p_{i,t}$ of vehicle i and $p_{j,t}$ of vehicle j at time $t \in \mathcal{T}$ has a non-convex nature written in the ℓ_2 norm: $\|p_{i,t} - p_{j,t}\|_2 \geq d$. It also can be written in an expansion form as the non-convex constraint (7). By defining:

$$\begin{cases} f_i(x) = d, & \text{convex expression} \\ -g_i(x) = -\|p_{i,t} - p_{j,t}\|_2, & \text{concave expression} \end{cases}$$

the non-convex constraint (7) is enforced in the CCP form.

On the one hand, considering three-dimensional view in Fig. 3a, the non-convex constraint (7) of the DCA model composes a sphere, while the constraint (11) of the MICP model constructs a cube. It can be seen that the sphere is snugly fitted in the cube. Consequently, the minimum safety margin between two vehicles $(i, j) \in \mathcal{N}$ of the MICP model is $2 \times d$ (the diagonal of a cube) at some time steps. Meanwhile the minimum safety margin of the DCA model always remains at d (the diameter of a sphere). Therefore, the fuel costs consumed by vehicles in the MICP model can be higher than in the DCA model. On the other hand, considering two-dimensional view (top view) in Fig. 3b, the minimum safety margin of the DCA model: $d\sqrt{2}$ (the diagonal of square) is larger than that of the MICP model: d (the diameter of circle).

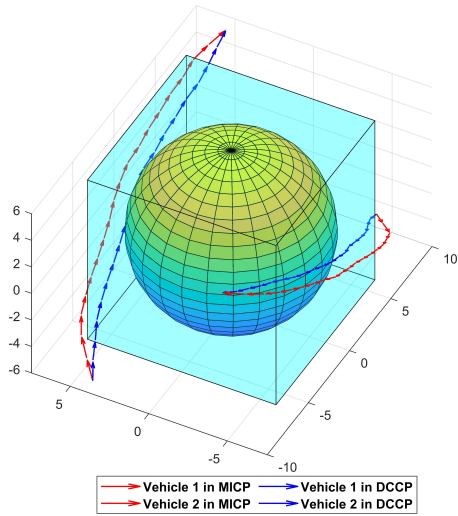
E. Convexified Non-convex collision avoidance constraint

Convexify the objective function and constraints with their affine approximations:

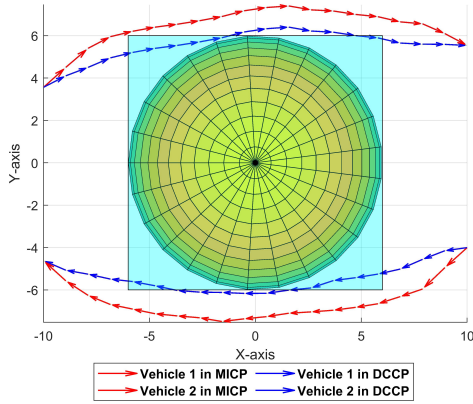
$$\hat{g}(x, x_k) = g(x_k) + \nabla g(x_k) (x - x_k) \quad (14)$$

VI. NUMERICAL RESULTS

We implemented the MICP model and DCA model on a PC configured by Intel Xeon and 32GB of RAM. To benchmark the performance of both models, we verify their formulation for 5, 10, and 15 vehicles with GUROBI solver. In the three numerical experiments, the minimum safety distance between vehicles $\forall (i, j) \in \mathcal{N}$ is $d = 5$ and the quantity of time steps is $\mathcal{T} = 30$. Fig. ?? and 4 show the data on the distance between



(a) Three-dimensional view



(b) Top view

Fig. 3. Illustration of the collision avoidance constraint in MICP model and DCA model for trajectory planning of two vehicles

vehicles at each time step $t \in \mathcal{T}$. In which, there are 10, 45, and 105 separations corresponding to number of pairs of vehicle for 5-vehicle, 10-vehicle, and 15-vehicle experiments, respectively.

There are three striking features needed to be elaborated from Fig. ?? and 4. Firstly, there is no crash between vehicles entire the time steps in both models in all three experiments. Secondly, more vehicles involved in operation lead to a reduction in distances between them in the same predetermined space. Thirdly, the larger collision-free space of MICP could remarkably reduce the feasible space for a global optimal solution than that of DCA. Additionally, as discussed in Section V-D the collision-free space of vehicles in DCA model is smaller than in MICP model. Therefore, the fuel cost of DCA is smaller than that of MICP as shown in Table. I.

As can be seen, Fig. 5 demonstrates the numerical proof of convergence for DCA in all test cases. The condition for DCA to converge to the global optimum at iteration k is both

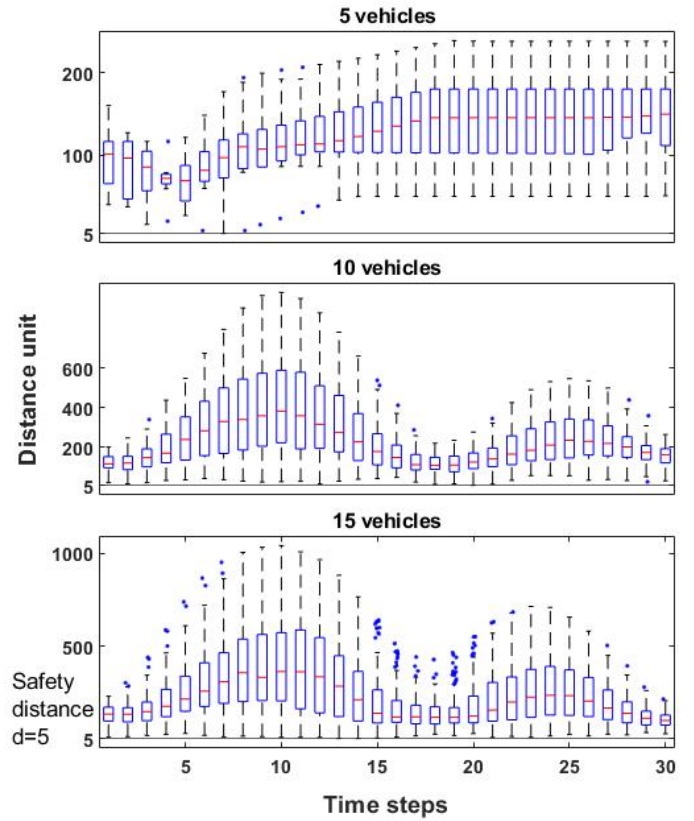


Fig. 4. Distance between vehicles DCA Model

the value of maximum slack variable s_i^k , and the gap value δ_k between objective function of sub-problem k and sub-problem $k + 1$ reach to 0. The optimal solutions of 5-vehicle, 10-vehicle, and 15-vehicle experiments are converged at iteration 34, 470, and 219, respectively. It should be remarked that the more number of iterations, which an experiment takes does not mean the longer computation time it would take. As the total computation time of a problem also relies on a solving process of every single sub-problem.

VII. CONCLUSION

In general, MICP and DCA arrive at the similar solutions for flight path generation on the fixed time steps horizon. However, the solutions of DCA takes an advantage over those of MICP in relations to the economical savings on fuel consumption as the collision-free space of the former is smaller than that of the latter. Therefore, DCA is particularly advantageous in a congested flying space. In addition, DCA is an iterative procedure, thus a proof of global convergence is crucial to prove the effectiveness of the algorithm to the trajectory optimization problem. Our work so far has been devoted to the global convergence of algorithm in all experiments.

ACKNOWLEDGEMENT

This work was supported in part by the Laboratory Directed Research and Development program at Sandia National Labo-

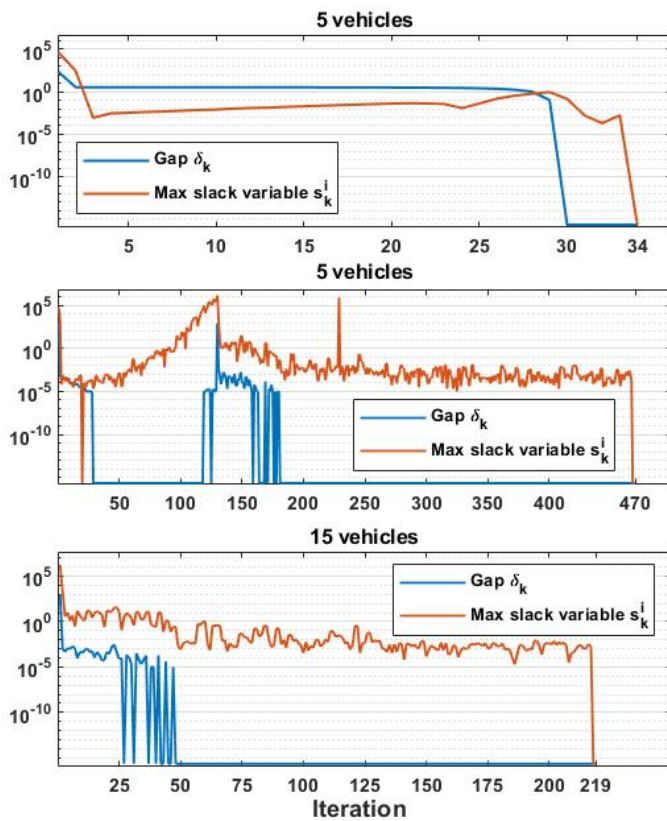


Fig. 5. Convergence analysis of DCA for experiments

ratories for the U.S. Department of Energy’s National Nuclear Security Administration under contract DE-NA0003525, and in part by the North Carolina A&T State University’s College of Engineering Intel Fellowship Program.

REFERENCES

- [1] D. Ioan, I. Prodan, S. Olaru, F. Stoican, and S.-I. Niculescu, “Mixed-integer programming in motion planning,” *Annual Reviews in Control*, vol. 51, pp. 65–87, 2021.
- [2] P. R. Chandler, M. Pachter, D. Swaroop, J. M. Fowler, J. K. Howlett, S. Rasmussen, C. Schumacher, and K. Nygard, “Complexity in uav cooperative control,” in *Proceedings of the 2002 American Control Conference*, vol. 3. IEEE, 2002, pp. 1831–1836.
- [3] P. Chandler, C. Schumacher, and S. Rasmussen, “Task allocation for wide area search munitions via network flow optimization,” in *AIAA Guidance, Navigation, and Control Conf. and Exh.*, 2001, p. 4147.
- [4] B. B. D. Luders, “Robust trajectory planning for unmanned aerial vehicles in uncertain environments,” Ph.D. dissertation, MIT, 2008.
- [5] J. M. Carson, B. Acikmeşe, L. Blackmore, and A. A. Wolf, “Capabilities of convex powered-descent guidance algorithms for pinpoint and precision landing,” in *2011 Aerospace Conf.* IEEE, 2011, pp. 1–8.
- [6] X. Shen, S. Diamond, Y. Gu, and S. Boyd, “Disciplined convex-concave programming,” in *2016 IEEE 55th Conference on Decision and Control (CDC)*. IEEE, 2016, pp. 1009–1014.
- [7] P. D. Tao and L. T. H. An, “Difference of convex functions optimization algorithms (dca) for globally minimizing nonconvex quadratic forms on euclidean balls and spheres,” *Operations Research Letters*, vol. 19, no. 5, pp. 207–216, 1996.
- [8] —, “A difference of convex optimization algorithm for solving the trust-region subproblem,” *SIAM Journal on Optimization*, vol. 8, no. 2, pp. 476–505, 1998.

- [9] L. T. H. An, P. D. Tao, and H. V. Ngai, “Exact penalty and error bounds in dc programming,” *Journal of Global Optimization*, vol. 52, no. 3, pp. 509–535, 2012.
- [10] T. Lipp and S. Boyd, “Variations and extension of the convex–concave procedure,” *Optimization and Eng.*, vol. 17, no. 2, pp. 263–287, 2016.
- [11] M. Grant, S. Boyd, and Y. Ye, “Disciplined convex programming,” in *Global optimization*. Springer, 2006, pp. 155–210.